Hindawi Publishing Corporation
EURASIP Journal on Advances in Signal Processing
Volume 2008, Article ID 352796, 12 pages
doi:10.1155/2008/352796

Research Article

Link-Adaptive Distributed Coding for Multisource Cooperation

Alfonso Cano, Tairan Wang, Alejandro Ribeiro, and Georgios B. Giannakis

Department of Electrical and Computer Engineering, University of Minnesota, 200 Union Street, Minneapolis, MN 55455, USA

Correspondence should be addressed to Georgios B. Giannakis, georgios@umn.edu

Received 14 May 2007; Accepted 7 September 2007

Recommended by Keith Q. T. Zhang

Combining multisource cooperation and link-adaptive regenerative techniques, a novel protocol is developed capable of achieving diversity order up to the number of cooperating users and large coding gains. The approach relies on a two-phase protocol. In Phase 1, cooperating sources exchange information-bearing blocks, while in Phase 2, they transmit reencoded versions of the original blocks. Different from existing approaches, participation in the second phase does not require correct decoding of Phase 1 packets. This allows relaying of soft information to the destination, thus increasing coding gains while retaining diversity properties. For any reencoding function the diversity order is expressed as a function of the rank properties of the distributed coding strategy employed. This result is analogous to the diversity properties of colocated multi-antenna systems. Particular cases include repetition coding, distributed complex field coding (DCFC), distributed space-time coding, and distributed error-control coding. Rate, diversity, complexity, and synchronization issues are elaborated. DCFC emerges as an attractive choice because it offers high-rate, full spatial diversity, and relaxed synchronization requirements. Simulations confirm analytically established assessments.

1. INTRODUCTION

In distributed virtual antenna arrays (VAA) enabled by user cooperation, there is a distinction as to how users decide to become part of the VAA for a given transmitted packet. Most relaying techniques can be classified either as analog forwarding (AF), decode-and-forward (DF), and selective forwarding (SF) [1–3]. In SF, prospective cooperators decode each source packet and, if correctly decoded, they cooperate by relaying a possibly reencoded signal. In AF, cooperating terminals amplify the received (transmitted signal plus noise) waveform. Both strategies achieve full diversity equal to the number of users forming the VAA, and in some sense their advantages and drawbacks are complementary. One of the major limitations of AF is that it requires storage of the analog-amplitude received waveform, which strains resources at relaying terminals, whereas SF implementation is definitely simpler. However, relaying information in SF is necessarily done on a per-packet basis eventually leading to the dismissal of an entire packet because of a small number of erroneously decoded symbols. This drawback is sometimes obscured in analyses because it does not affect the diversity gain of the VAA. It does affect the coding gain, though, and in many situations, SF does not improve performance of noncooperative transmissions because the diversity advantage requires too high signal-to-noise ratios (SNR) to "kick-in" in practice [4].

Simple implementation with high diversity and coding gains is possible with the DF-based link-adaptive regenerative (LAR) cooperation, whereby cooperators repeat packets based on the instantaneous SNR of the received signal [4]. In LAR cooperation, relays retransmit soft estimates of received symbols with power proportional to the *instantaneous* SNR in the source-to-relay link—available through, for example, training—but never exceeding a given function of the *average* SNR in the relay-to-destination link which is available through, for example, low-rate feedback. With LAR-based cooperation, it suffices to perform maximum-ratio combining (MRC) at the destination to achieve full diversity equal to the number of cooperators [4]. Finally, link-adaptive cooperation was also considered for power-allocation purposes, as in [5, 6], and references therein.

In the present paper, we extend LAR cooperation to general distributed coding strategies operating over either orthogonal or nonorthogonal channels. For that matter, we consider a multisource cooperation (MSC) setup, whereby a group of users collaborate in conveying information symbols to a common destination [7, 8]. In Phase 1, terminals

sequentially transmit their information bearing signals. Due to the broadcast nature of wireless transmissions, signals are overheard by other terminals that use these received waveforms to estimate the information sent by other sources. In Phase 2, sources (re)encode the aggregate information packet that they then transmit to the destination. Combining the signals received during both phases, the destination estimates the sources data. The goal of this paper is to analyze the diversity of LAR-MSC protocols in terms of general properties of the reencoding function used during Phase 2. Particular cases of reencoding functions include (LAR based) (i) repetition coding, (ii) distributed complex field coding (DCFC), (iii) distributed space-time (ST) coding, and (iv) distributed error control coding (DECC).

The use of coding techniques (i)–(iv) in SF relaying has been considered in, for example, [8–12], where different diversity properties are reported. The use of repetition coding as in (i) with average SNR source-relay knowledge at the receivers was tackled in [9] using a piecewise linear (PL) detector that established diversity bounds. Alamouti codes [13] were considered as in (iii) with regenerative relays in [10, 11]. In particular, full diversity was demonstrated in [11] if the *per-fading* error probability of the relay can become available at the destination. DCFC and DECC cooperation in a multiple access channel, using a 2-phase protocol similar to the one proposed here in (ii) and (iv), was advocated by [8, 12], respectively. Assuming that to participate in the Phase 2, sources have to correctly decode the packets of all other peers, diversity order as high as the number of cooperating terminals was established.

In general terms, the present work differs from existing alternatives in that LAR cooperation is employed to enable high error performance (in coding gain and diversity) even if packets are not correctly decoded and realistic channel knowledge is available at terminals and destination. Our main result is to show that the diversity order of LAR-MSC coincides with that of a real antenna array using the same encoding function used by the VAA created by MSC. In particular, this establishes that for a network with N users, the diversity orders are (i) 2 for repetition coding, (ii) N for DCFC, (iii) at least the same diversity order afforded by the ST code in a conventional antenna array when we use distributed ST coding, and (iv) for DECC, the same diversity achieved by the ECC over an N-lag block fading channel. Through simulations we also corroborate that, having the same diversity gain, LAR transmissions enable higher coding gains than those afforded by SF-based transmissions.

The rest of the paper is organized as follows. In Section 2, we introduce the 2-phase LAR-MSC protocol. We define a generic encoding function and specialize it to repetition coding and DCFC. We then move on to Section 3 where we present the main result of the paper characterizing the diversity gain in terms of the properties of the distributed coder. We discuss the application of our result to repetition coding, DCFC, distributed ST coding, and DECC in Section 3.2. In this section, we also compare these four different strategies in terms of diversity, decoding complexity, synchronization, and bandwidth efficiency. Section 3.1 is devoted to prove the main result introduced in Section 3. We present corroborating simulations in Section 4.

Notation 1. Upper (lower) bold face letters will be used for matrices (column vectors); $[\cdot]_{i,j}$ ($[\cdot]_i$) for the i, jth (ith) entry of a matrix (vector); $[\cdot]_{i,:}$ ($[\cdot]_{:,j}$) for the ith (jth) row (column) of a matrix; $[\cdot]_{i:j}$ will denote a vector formed extracting elements from i to j; $\mathbf{I}_N$ the $N \times N$ identity matrix; $\mathbf{1}_N$ the $N \times 1$ all-one vector; $\otimes$ the Kroneker product; $\|\cdot\|$ the Frobenius norm; $\mathcal{R} \cup \mathcal{S}$ ($\mathcal{R} \cap \mathcal{S}$) the union (intersection) of sets $\mathcal{R}$ and $\mathcal{S}$; $|\mathcal{S}|$ the cardinality of a set $\mathcal{S}$; $\varnothing$ the empty set; and $\mathcal{CN}(\mu, \sigma^2)$ will stand for a complex Gaussian distribution with mean μ and variance σ^2.

2. LINK-ADAPTIVE REGENERATIVE MULTI-SOURCE COOPERATION

Consider a set of sources $\{S_n\}_{n=1}^N$ communicating with a common access point or destination S_{N+1}. Information bits of S_n are modulated and parsed into $K \times 1$ blocks of symbols $\mathbf{x}_n := [x_{n1}, \ldots, x_{nK}]^T$ with x_{nk} drawn from a finite alphabet (constellation) $\mathcal{A}_s$. Terminals cooperate in accordance to a two-phase protocol. In Phase 1, sources $\{S_n\}_{n=1}^N$ transmit their symbols to the destination S_{N+1} in nonoverlapping time slots. Thanks to broadcast propagation, symbols transmitted by S_n are also received by the other $N-1$ sources $\{S_m\}_{m=1,m\neq n}^N$; see also Figure 1. Let $\mathbf{y}_n^{(m)}$ represent the $K \times 1$ block received at S_m, $m \in [1, N+1]$, $m \neq n$ from S_n, $n \in [1, N]$. The $S_n \to S_m$ link is modeled as a block Rayleigh fading channel with coefficients $h_n^{(m)} \sim \mathcal{CN}(0, (\sigma_n^{(m)})^2 \overline{\gamma})$. Defining normalized additive white Gaussian noise (AWGN) terms $\mathbf{w}_n^{(m)} \sim \mathcal{CN}(0, \mathbf{I}_K)$ for the $S_n \to S_m$ link, we can write the Phase-1 input-output relations as

$$\mathbf{y}_n^{(m)} = h_n^{(m)} \mathbf{x}_n + \mathbf{w}_n^{(m)}, \quad m \in [1, N+1],\ n \in [1, N],\ n \neq m, \tag{1}$$

where we recall $m = N+1$ denotes the signal received at the common destination S_{N+1}. For reference, we also define the instantaneous output SNR of each link $\gamma_n^{(m)} := |h_n^{(m)}|^2$ and the corresponding average SNR as $\overline{\gamma}_n^{(m)} = (\sigma_n^{(m)})^2 \overline{\gamma}$ [cf. $h_n^{(m)} \sim \mathcal{CN}(0, (\sigma_n^{(m)})^2 \overline{\gamma})$].

After Phase 1, each source has available an estimate of the other sources blocks. Let $\hat{\mathbf{x}}_n^{(m)}$ denote the estimate of the source block $\mathbf{x}_n$ formed at source S_m, $m \in [1, N]$, $m \neq n$. Due to communication errors, $\hat{\mathbf{x}}_n^{(m)}$ will generally differ from the original block $\mathbf{x}_n$ and from estimates $\hat{\mathbf{x}}_n^{(l)}$ at different sources $S_l \neq S_m$.

In Phase 2, each source transmits to the destination a block that contains coded information from other sources' blocks. To be precise, consider the set of Phase-1 transmitted blocks, $:= \{\mathbf{x}_n\}_{n=1}^N$. If x were perfectly known at S_m, it *would* have been possible to form a reencoded block $\mathbf{v}_m$ of size $L \times 1$ obtained from x through a mapping $\mathcal{M}_m$, that is,

$$\mathbf{v}_m = \mathcal{M}_m(x). \tag{2}$$

Note, however, that x is not necessarily known at S_m. In fact, source S_m collects all estimates $\{\hat{\mathbf{x}}_n^{(m)}\}_{n=1,n\neq m}^N$ plus its own

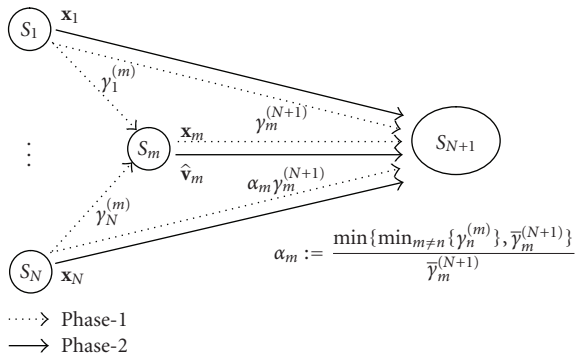

FIGURE 1: Transmitted and received signals at S_m during Phase 1 and Phase 2.

information $\mathbf{x}_m$ in the set $\hat{x}^{(m)} := \{\mathbf{x}_m, \{\hat{\mathbf{x}}_n^{(m)}\}_{n=1,n\neq m}^N\}$. The $L \times 1$ vector $\hat{\mathbf{v}}_m$ built by S_m in Phase 2 is thus obtained from $\hat{x}^{(m)}$ as

$$\hat{\mathbf{v}}_m = \mathcal{M}_m(\hat{x}^{(m)}). \tag{3}$$

Comparing (2) with (3) we see that different from the MSC strategies in [7, 14], we are encoding based on a set of error-corrupted blocks $\hat{x}^{(m)}$. To make this explicit, we denoted the mapped block as $\hat{\mathbf{v}}_m$ [cf. (3)] to emphasize that it may be different from the desired $\mathbf{v}_m$ [cf. (2)].

Propagation of decoding errors can have a detrimental effect on error performance at the destination. To mitigate this problem, our approach is to have source S_m adjust its Phase-2 transmitted power using a channel-adaptive scaling coefficient α_m. The block transmitted from S_m in Phase 2 is thus $\sqrt{\alpha_m}\,\hat{\mathbf{v}}_m$. The signal $\mathbf{y}^{(N+1,2)}$ received at the destination S_{N+1} is the superposition of the N source signals; see Figure 2. Upon defining a matrix of transmitted blocks $\hat{\mathbf{V}} := [\hat{\mathbf{v}}_1, \ldots, \hat{\mathbf{v}}_N] = [\mathcal{M}_1(\hat{x}^{(1)}), \ldots, \mathcal{M}_N(\hat{x}^{(N)})]$, a diagonal matrix containing the α_m coefficients $\mathbf{D}_\alpha := \text{diag}([\sqrt{\alpha_1}, \ldots, \sqrt{\alpha_N}])$ and the aggregate channel $\mathbf{h}^{(N+1)} := [h_1^{(N+1)}, \ldots, h_N^{(N+1)}]^T$ containing the coefficients from all sources to the destination, we can write

$$\mathbf{y}^{(N+1,2)} = \hat{\mathbf{V}}\mathbf{D}_\alpha\mathbf{h}^{(N+1)} + \mathbf{w}^{(N+1,2)}. \tag{4}$$

The destination estimates the set of transmitted blocks x using the N blocks of K symbols $\mathbf{y}_n^{(N+1,1)}$ received during Phase 1 and the L symbols $\mathbf{y}^{(N+1,2)}$ received during Phase 2. Assuming knowledge of the product $\mathbf{D}_\alpha\mathbf{h}^{(N+1)}$ (through, e.g., a training phase), demodulation at the destination relies on the detection rule

$$\hat{x} = \arg\min_{x\in\mathcal{A}_s^{KN}} \left\{ \sum_{n=1}^{N} \left\| \mathbf{y}_n^{(N+1,1)} - \text{diag}(\mathbf{x}_n)\mathbf{h}^{(N+1)} \right\|^2 + \left\| \mathbf{y}^{(N+1,2)} - \mathbf{V}\mathbf{D}_\alpha\mathbf{h}^{(N+1)} \right\|^2 \right\}, \tag{5}$$

where $\mathbf{V} := [\mathbf{v}_1, \ldots, \mathbf{v}_N] = [\mathcal{M}_1(x), \ldots, \mathcal{M}_N(x)]$. The search in (5) is performed over the set of constellation codewords x with size $|\mathcal{A}_s|^{KN}$. Note that this is a general detector for performance analysis purposes but its complexity does not necessarily depend on the size of the set x; see also Section 4.

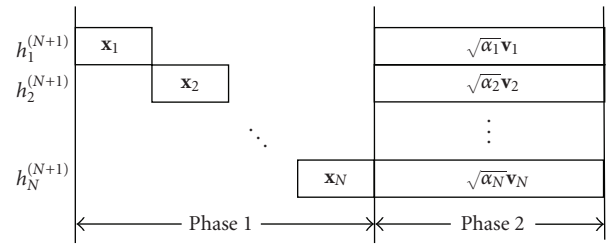

FIGURE 2: Time-division scheduling for N sources during Phase 1 and simultaneous transmissions during Phase 2.

The goal of this paper is to characterize the diversity of the 2-phase MSC protocol with input/output relations (1) and (4) and detection rule (5) in terms of suitable properties of the mappings $\mathcal{M}_m$. In particular, we will show that for given mappings $\mathcal{M}_m$, an appropiate selection of the coefficients $\mathbf{D}_\alpha$ enables diversity order equal to an equivalent multi-antenna system with N colocated transmit antennas; that is, when no inter-source error occurs. Purposefully general, to illustrate notation, let us describe two examples for $\mathcal{M}_m$ yielding different MSC protocols.

Example 1 (repetition coding). A simple cooperation strategy for Phase 2 is that each source retransmits the packet of one neighbor; that is, if we build a mapping

$$\mathcal{M}_m: \ \mathbf{v}_m = \left[\mathbf{0}_{(\tilde{m}-1)P}^T, \mathbf{x}_{\tilde{m}}^T, \mathbf{0}_{(N-\tilde{m})P}^T\right]^T \tag{6}$$

with $\tilde{m} = \text{mod}[m, N]+1$, the mth terminal repeats the $m-1$)st signal's estimate for $m\neq 1$ and the first terminal repeats the Nth signal's estimate. Note that the all-zero vectors appended before and after $\mathbf{x}_{\tilde{m}}^T$ are to separate transmissions in time during Phase 2. With this definition, it can be seen that the optimum receiver in (5) simplifies for each entry k to

$$[\hat{\mathbf{x}}_m^{(N+1)}]_k = \arg\min_{x\in\mathcal{A}_s} \left\{ \left| \left[\mathbf{y}_m^{(N+1,1)}\right]_k - h_m^{(N+1)}x \right|^2 + \left| \left[\mathbf{y}^{(N+1,2)}\right]_{(\tilde{m}+1)K+k} - \sqrt{\alpha_{\tilde{m}}}h_{\tilde{m}}^{(N+1)}x \right|^2 \right\}. \tag{7}$$

Example 2 (distributed complex-field coding). Define the $N\times 1$ column vector $\mathbf{p}_k^{(m)} := [[\mathbf{x}_1^{(m)}]_k, \ldots, [\mathbf{x}_m]_k, \ldots, [\mathbf{x}_N^{(m)}]_k]^T$ and linearly code it using a row $1 \times N$ vector $\boldsymbol{\theta}_m^T$, taken as the mth row of a complex-field coding matrix $\boldsymbol{\Theta}$ [15]. Repeating this process for all k, the mapping $\mathcal{M}_m$ now becomes

$$\mathcal{M}_m: \ \mathbf{v}_m = \left[\mathbf{0}_{(m-1)P}^T, \boldsymbol{\theta}_m^T\left[\mathbf{p}_1^{(m)}, \ldots, \mathbf{p}_K^{(m)}\right], \mathbf{0}_{(N-m)P}^T\right]^T. \tag{8}$$

In this case, the destination S_{N+1} can decode $\mathbf{p}_k^{(m)}$ using the following detection rule:

$$\hat{\mathbf{p}}_k^{(N+1)} = \arg\min_{\mathbf{p}_k\in\mathcal{A}_s^N} \left\{ \left\| \mathbf{q}_k^{(N+1,1)} - \text{diag}(\mathbf{p}_k)\mathbf{h}^{(N+1)} \right\|^2 + \left\| \mathbf{q}_k^{(N+1,2)} - \text{diag}(\boldsymbol{\Theta}\mathbf{p}_k)\mathbf{D}_\alpha\mathbf{h}^{(N+1)} \right\|^2 \right\}, \tag{9}$$

where $\mathbf{q}_k^{(N+1,1)} := [[\mathbf{y}_1^{(N+1,1)}]_k, \ldots, [\mathbf{y}_N^{(N+1,1)}]_k]^T$ and $\mathbf{q}_k^{(N+1,2)} := [[\mathbf{y}^{(N+1,2)}]_{(k-1)N+1}, \ldots, [\mathbf{y}_N^{(N+1,2)}]_{kN}]^T$.

3. ERROR-PROBABILITY ANALYSIS

The purpose of this section is to determine the high-SNR diversity order of MSC protocols in terms of suitable properties of the mapping $\mathcal{M}_m$. For given channels $\mathcal{H}^{(d)} := \{h_n^{(N+1)}\}_{n=1}^N$ from sources to destination and $\mathcal{H}^{(s)} := \{h_n^{(m)}\}_{m,n=1,m\neq n}^N$ between sources, we define the so-called conditional (or instantaneous) pairwise error probability (PEP) $\Pr\{x\neq\hat{x} \mid \mathcal{H}^{(s)}, \mathcal{H}^{(d)}\}$ as the probability of decoding $\tilde{x}$ when x was transmitted and denoted as $\Pr\{x \to \tilde{x} \mid \mathcal{H}^{(s)}, \mathcal{H}^{(d)}\}$. The diversity order of the MSC protocol is defined as the slope of the logarithm of the average PEP as the SNR goes to infinity, that is,

$$d = \min_{x,\tilde{x}\neq x}\left\{ -\lim_{\overline{\gamma}\to\infty} \frac{\log \mathrm{E}[\Pr\{x \longrightarrow \tilde{x} \mid \mathcal{H}^{(s)}, \mathcal{H}^{(d)}\}]}{\log \overline{\gamma}} \right\}. \quad (10)$$

For MIMO block-fading channels, the diversity order d depends on the rank distance between constellation codewords [16]. This will turn out to be generalizable to the VAA created in LAR-MSC systems. For that matter, define the set

$$\mathcal{X} := \{n \mid \mathbf{x}_n - \tilde{\mathbf{x}}_n \neq 0\} \quad (11)$$

containing the indices of the sources transmitting different packets. For the same x and $\tilde{x}$ consider the corresponding phase-2 blocks $\mathbf{V}$ and $\tilde{\mathbf{V}}$. We are interested in a subset of columns of $(\mathbf{V} - \tilde{\mathbf{V}})$ that form a basis of the span of its columns. This can be formally defined as

$$\mathcal{V} := \{n \mid \mathrm{span}(\{\mathbf{v}_n - \tilde{\mathbf{v}}_n\}_{n\in\mathcal{V}}) = \mathrm{span}(\mathbf{V} - \tilde{\mathbf{V}})\}, \quad (12)$$

where $\mathrm{span}(\cdot)$ denotes the span of a set of vectors or columns of a matrix. With reference to Figure 2, if we assume $\hat{\mathbf{V}} = \mathbf{V}$, the equivalent system can be seen as a MISO block-faded transmission and the achievable diversity order is related to $\mathrm{rank}(\mathbf{V} - \tilde{\mathbf{V}}) = |\mathcal{V}|$ over all possible pairs, where $\mathrm{rank}(\cdot)$ denotes the rank of a matrix. We are now challenged to establish similar diversity claims when $\hat{\mathbf{V}}\neq\mathbf{V}$ along with the contribution to diversity of $\mathcal{X}$ after Phase 1. The pertinent result is summarized in the following theorem we prove in Section 3.1.

Theorem 1. *Consider two distinct blocks $x, \tilde{x}$ and the pairwise-error indicator sets $\mathcal{X}$ and $\mathcal{V}$ defined in* (11) *and* (12)*, respectively. Let the Phase-2 power-weighting coefficients $\{\alpha_n\}_{n=1}^N$ be*

$$\alpha_m := \frac{\min\{\min_{m\neq n}\{\gamma_n^{(m)}\}, \overline{\gamma}_m^{(N+1)}\}}{\overline{\gamma}_m^{(N+1)}}, \quad (13)$$

where $\gamma_n^{(m)}\,\overline{\gamma}_m^{(N+1)}$ is the instantaneous (average) SNR of link $S_n - S_m$ ($S_m - S_{N+1}$), $m \in [1, N]$. The average diversity order as defined in (10) *of the MSC protocol defined in* (1)–(5) *is*

$$d = \min_{x,\tilde{x}\neq x}\left\{ -\lim_{\overline{\gamma}\to\infty} \frac{\log \Pr\{x \longrightarrow \tilde{x}\}}{\log \overline{\gamma}} \right\} = \min_{x,\tilde{x}\neq x}\{|\mathcal{X} \cup \mathcal{V}|\}. \quad (14)$$

The coefficient α_m in (13) is formed based on the instantaneous SNR of the links through which blocks $\{\mathbf{y}_n^{(m)}\}_{n=1,n\neq m}^N$ arrived (available, e.g., by appending a training sequence) and the average SNR of its link to the destination, which is assumed to slowly fade at long scale, and thus is feasible to be fed back. These same conventions have also been adopted in the context of DF protocols in [4, 9]. In [9], the average channel is assumed to be known for decoding at the destination, whereas in [4] average knowledge is assumed to be known at the relays; the latter has been proved to be full-diversity achieving, while the former cannot achieve full-diversity, which in our set-up amounts to N, the number of sources transmitting to the destination.

As detailed in the next subsection, the diversity order can be assessed by establishing proper bounds on the PEP as in, for example, [9] or [4]. However, for systems with the same diversity order, comparing relative performance typically relies on their respective coding gains [17, Chapter 2]. Unfortunately, analytical assessment of coding gains is rarely possible in closed form especially for the DF-based cooperative systems even for simple constellations using repetition coding; see also [9] for similar comments. For this reason, we will resort to simulated tests in order to assess coding-gain performance in Section 4.

3.1. Proof of Theorem 1

The difficulty in proving Theorem 1 is the possibility of having decoding errors between cooperating terminals, that is, $\hat{x}^{(m)}\neq x$. Thus, define the set of sources' indices that estimate x erroneously,

$$\mathcal{E} := \{m \mid x\neq\hat{x}^{(m)}\}. \quad (15)$$

By definition $\mathcal{E}$'s complement $\overline{\mathcal{E}}$ contains the indices of the sources that decoded x correctly. For a given set $\overline{\mathcal{E}}$ of correct decoders, one expects that sources $\{S_m\}_{m\in\overline{\mathcal{E}}}$ help to increase the detection probability, whereas sources $\{S_m\}_{m\in\mathcal{E}}$ tend to decrease it.

In terms of diversity, not all of the elements of $\overline{\mathcal{E}}$ contribute to increasing its order. In fact, for S_m to contribute to the diversity order it also has to belong to the set $(\mathcal{X} \cup \mathcal{V})$. Thus, we define the set

$$\mathcal{C} := (\mathcal{X} \cup \mathcal{V}) \cap \overline{\mathcal{E}}. \quad (16)$$

The cardinality of $\mathcal{C}$ can be bounded as $|\mathcal{C}| \geq |\mathcal{X} \cup \mathcal{V}| - |\mathcal{E}|$. Note also that $\mathcal{C} \cap \mathcal{E} = \varnothing$.

Using these definitions, we can condition on the set of correct decoders $\overline{\mathcal{E}}$ and bound (i) the probability $\Pr\{x \to \{\hat{x}^{(m)}\}_{m=1}^N \mid \mathcal{H}^{(s)}\}$ of erroneous detection at the sources after Phase 1; and (ii) the probability $\Pr\{x, \{\hat{x}^{(m)}\}_{m=1}^N \to \tilde{x} \mid \mathcal{H}^{(s)}, \mathcal{H}^{(d)}\}$ of incorrect detection at the destination after Phase 1 and Phase 2. The result is stated in the following lemma.

Lemma 1. *Consider a transmitted block x, a set of estimated blocks $\{\hat{x}^{(m)}\}_{m=1}^N$ at terminals $\{S_m\}_{m=1}^N$, and an estimated block $\tilde{x}$ at the destination. Let* (i) *$\mathcal{E}$ and $\mathcal{C}$ denote the sets defined in*

(15) *and* (16); (ii) *let* $\gamma_n^{(m)} = |h_n^{(m)}|^2$ *and* $\gamma_n^{(N+1)} = |h_n^{(N+1)}|^2$ *be the instantaneous SNRs in the* $S_n \to S_m$ *and* $S_n \to S_{N+1}$ *links; and* (iii) *let* α_m *denote the power scaling constant in* (13). *Conditioned on fading realizations,*

(a) *the conditional probability of decoding* $\{\hat{x}^{(m)}\}_{m=1}^N$ *at* $\{S_m\}_{m=1}^N$ *given that* x *was transmitted in Phase-1 can be bounded as*

$$\Pr\left\{x \longrightarrow \{\hat{x}^{(m)}\}_{m=1}^N \mid \mathcal{H}^{(s)}\right\} \leq \kappa_1 \exp\left(-\kappa_2 \sum_{n\in\mathcal{E}} \min_{m\neq n}\{\gamma_n^{(m)}\}\right) \tag{17}$$

for some finite constants κ_1, κ_2;

(b) *the conditional probability of detecting* $\widetilde{x}$ *given that* x *was transmitted in Phase-1 and* $\{\hat{x}^{(m)}\}_{m=1}^N$ *in Phase-2 is bounded as*

$$\Pr\left\{x, \{\hat{x}^{(m)}\}_{m=1}^N \longrightarrow \widetilde{x} \mid \mathcal{H}^{(s)}, \mathcal{H}^{(d)}\right\} \leq Q\left(\frac{\kappa_3 \sum_{n\in\mathcal{C}} \alpha_n \gamma_n^{(N+1)} - \kappa_4 \sum_{n\in\mathcal{E}} \alpha_n \gamma_n^{(N+1)}}{\sqrt{\kappa_3 \sum_{n\in\mathcal{C}} \alpha_n \gamma_n^{(N+1)} + \kappa_4 \sum_{n\in\mathcal{E}} \alpha_n \gamma_n^{(N+1)}}}\right) \tag{18}$$

for some finite constants κ_3, κ_4.

Proof. See Appendices A and B. □

Using results (a) and (b) of Lemma 1, we can bound the PEP in (10) to obtain

$$\Pr\{x \longrightarrow \widetilde{x} \mid \mathcal{H}^{(s)}, \mathcal{H}^{(d)}\} \leq \sum_{\forall \{\hat{x}^{(m)}\}_{m=1}^N} \kappa_1 \exp\left(-\kappa_2 \sum_{n\in\mathcal{E}} \min_{m\neq n}\{\gamma_{m,n}^{(s)}\}\right) \times Q\left(\frac{\kappa_3 \sum_{n\in\mathcal{C}} \alpha_n \gamma_n^{(N+1)} - \kappa_4 \sum_{n\in\mathcal{E}} \alpha_n \gamma_n^{(N+1)}}{\sqrt{\kappa_3 \sum_{n\in\mathcal{C}} \alpha_n \gamma_n^{(N+1)} + \kappa_4 \sum_{n\in\mathcal{E}} \alpha_n \gamma_n^{(N+1)}}}\right). \tag{19}$$

To interpret the bound in (19) let us note that the factors in (17) and (18) are reminiscent of similar expressions that appear in error-probability analysis of fading channels [18, Chapter 14]. Taking expected values over the complex Gaussian distribution of the channels in $\mathcal{H}^{(s)}$ and $\mathcal{H}^{(d)}$ allows us to bound the right-hand side of (17) as

$$\mathrm{E}\left[\exp\left(-\kappa_2 \sum_{n\in\mathcal{E}} \min_{m\neq n}\{\gamma_n^{(m)}\}\right)\right] \leq (k_1\overline{\gamma})^{-|\mathcal{E}|} \tag{20}$$

for some constant k_1. With respect to (18), we expect decoding errors at S_n when some of the fading coefficients $\{\gamma_n^{(m)}\}_{m\neq n}$ are small. In turn, since $\alpha_n \leq \min_{m\neq n}\{\gamma_n^{(m)}\}$ we expect $\sum_{n\in\mathcal{E}} \alpha_n \gamma_n^{(N+1)}$ to be small since $n \in \mathcal{E}$ when decoding errors are present at S_n. Thus, the right-hand side of (18) can be approximated as

$$Q\left(\frac{\kappa_3 \sum_{n\in\mathcal{C}} \alpha_n \gamma_n^{(N+1)} - \kappa_4 \sum_{n\in\mathcal{E}} \alpha_n \gamma_n^{(N+1)}}{\sqrt{\kappa_3 \sum_{n\in\mathcal{C}} \alpha_n \gamma_n^{(N+1)} + \kappa_4 \sum_{n\in\mathcal{E}} \alpha_n \gamma_n^{(N+1)}}}\right) \approx Q\left(\sqrt{\kappa_3 \sum_{n\in\mathcal{C}} \alpha_n \gamma_n^{(N+1)}}\right). \tag{21}$$

As is well known [18, Chpater 14], the expected value of the right-hand side of (21) can be bounded as

$$\mathrm{E}\left[Q\left(\sqrt{\kappa_3 \sum_{n\in\mathcal{C}} \alpha_n \gamma_n^{(N+1)}}\right)\right] \leq (k_2\overline{\gamma})^{-|\mathcal{C}|} \tag{22}$$

for some constant k_2.

Combining (22), (20), and (19), we could deduce that $\Pr\{x \to \widetilde{x}\} := \mathrm{E}[\Pr\{x \to \widetilde{x} \mid \mathcal{H}^{(s)}, \mathcal{H}^{(d)}\}] \leq (k_1 k_2 \overline{\gamma})^{-|\mathcal{C}|-|\mathcal{E}|}$. Since $|\mathcal{C}| \geq |\mathcal{X} \cup \mathcal{V}| - |\mathcal{E}|$, we have $|\mathcal{C}| + |\mathcal{E}| \geq |\mathcal{X} \cup \mathcal{V}|$, which establishes Theorem 1. This argument is not a proof however, since (22) is a bound on the approximation (21). Furthermore, the factors in the products of (19) are dependent through $\alpha_m := \min\{\min_{m\neq n}\{\gamma_n^{(m)}\}, \overline{\gamma}_m^{(N+1)}\}/\overline{\gamma}_m^{(N+1)}$ [cf. (13)] and cannot be factored into a product of expectations. The next lemma helps us to overcome these technical difficulties.

Lemma 2. *For some error probability* $P_e'\{\gamma_c, \gamma_e, \eta_c, \eta_e\}$ *satisfying*

$$P_e'\{\gamma_c, \gamma_e, \eta_c, \eta_e\} \leq \kappa_1 \exp(-\kappa_2\gamma_e) Q\left[\frac{\kappa_3\gamma_c\eta_c - \kappa_4\gamma_e\eta_e}{\kappa_3\sqrt{\gamma_c\eta_c + \kappa_4\gamma_e\eta_e}}\right] \tag{23}$$

for some finite constants $\kappa_1, \kappa_2, \kappa_3, \kappa_4$, *and* $\gamma_c \sim$ *Gamma* $(|\mathcal{C}|, 1/\overline{\gamma})$, $\gamma_e \sim$ *Gamma* $(|\mathcal{E}|, 1/\overline{\gamma})$; γ_c, η_c, γ_e, *and* η_e *are nonnegative and independent of each other, if the probability density functions* $p(\eta_c)$ *and* $p(\eta_e)$ *do not depend on* $\overline{\gamma}$, *the expectation over* γ_c, γ_e, η_c, *and* η_e *is bounded as*

$$P_e' \leq (k\overline{\gamma})^{-|\mathcal{C}|-|\mathcal{E}|} \tag{24}$$

with $k := \mathrm{E}[k(\eta_c, \eta_e)]$ *a constant not dependent on* $\overline{\gamma}$.

Proof. See [19]. □

Combining Lemmas 1 and 2, we can prove Theorem 1 as we show next.

Proof of Theorem 1. Using the definition of α_m in (13), one can derive the following bounds on the probability expressed in (19):

$$\begin{aligned}
\sum_{n\in\mathcal{E}} \alpha_n \gamma_n^{(N+1)} &= \sum_{n\in\mathcal{E}} \frac{\min\{\min_m\{\gamma_n^{(m)}\}, \overline{\gamma}\}}{\overline{\gamma}} \gamma_n^{(N+1)} \\
&\leq \left(\sum_{n\in\mathcal{E}} \min_m\{\gamma_n^{(m)}\}\right) \frac{\sum_{n\in\mathcal{E}} \gamma_n^{(N+1)}}{\overline{\gamma}}, \\
\sum_{n\in\mathcal{C}} \alpha_n \gamma_n^{(N+1)} &= \left(\sum_{n\in\mathcal{C}} \gamma_n^{(N+1)}\right) \times \left[\sum_{n\in\mathcal{C}} \frac{\min\{\min_m\{\gamma_n^{(m)}\}, \overline{\gamma}\}}{\overline{\gamma}} \frac{\gamma_n^{(N+1)}}{\sum_{n\in\mathcal{C}} \gamma_n^{(N+1)}}\right] \\
&\geq \left(\sum_{n\in\mathcal{C}} \gamma_n^{(N+1)}\right) \frac{\min\{\min_{\forall m,n\in\mathcal{C}}\{\gamma_n^{(m)}\}, \overline{\gamma}\}}{\overline{\gamma}},
\end{aligned} \tag{25}$$

where we set all instantaneous SNRs to have the same average $\overline{\gamma}$; that is, one can pick the maximum average SNR among all

links of our setup and bound the performance of this system by another one with the same average SNR $\overline{\gamma}$ in all links, as demonstrated in [19].

If one defines $\gamma_e := \sum_{n\in\mathcal{E}} \min_n\{\gamma_n^{(m)}\}$, $\gamma_c := \sum_{n\in\mathcal{C}} \gamma_n^{(N+1)}$, $\eta_e := \min\{\min_{\forall m,n\in\mathcal{C}}\{\gamma_n^{(m)}\}, \overline{\gamma}\}/\overline{\gamma}$ and $\eta_c := \sum_{n\in\mathcal{E}} \gamma_n^{(N+1)}/\overline{\gamma}$, then we obtain the upper bound

$$\Pr\{x \longrightarrow \widetilde{x} \mid \mathcal{H}^{(s)}, \mathcal{H}^{(d)}\} \leq \sum_{\forall\{\hat{x}^{(m)}\}_{m=1}^{N}} \kappa_1 \exp(-\kappa_2\gamma_e) Q\left[\frac{\kappa_3\gamma_c\eta_c - \kappa_4\gamma_e\eta_e}{\sqrt{\kappa_3\gamma_c\eta_c + \kappa_4\gamma_e\eta_e}}\right], \tag{26}$$

where $\gamma_c^{(d)} \sim \text{Gamma}(|\mathcal{C}|, 1/\overline{\gamma})$, $\gamma_e^{(s)} \sim \text{Gamma}(|\mathcal{E}|, (N-1)/\overline{\gamma})$; $\gamma_c^{(d)}$, η_c, $\gamma_e^{(s)}$, and η_e are nonnegative and independent of each other; that is,

$$\begin{aligned} &p(\eta_c) = \frac{\eta_e^{(|\mathcal{E}|-1)}}{(|\mathcal{E}|-1)!}\exp(-\eta_e),\\ &\eta_c = 1 \quad \text{with } \Pr\left(\min_{\forall m,n\in\mathcal{C}} \gamma_n^{(m)} \geq \overline{\gamma}\right) = \exp(-|\mathcal{C}|(N-1)),\\ &p(\eta_c) = |\mathcal{C}|(N-1)\exp(-|\mathcal{C}|(N-1)\eta_e) \quad \text{with } \Pr\left(\min_{\forall m,n\in\mathcal{C}} \gamma_n^{(m)} < \overline{\gamma}\right) = 1-\exp(-|\mathcal{C}|(N-1)). \end{aligned} \tag{27}$$

Finally, because $|\mathcal{C}| \geq |\mathcal{X}\cup\mathcal{V}| - |\mathcal{E}|$, we have

$$\begin{aligned} \Pr\{x \longrightarrow \widetilde{x}\} &\leq \sum_{\forall\{\hat{x}^{(m)}\}_{m=1}^{N}} (k\overline{\gamma})^{-|\mathcal{C}|-|\mathcal{E}|}\\ &\leq \sum_{\forall\{\hat{x}^{(m)}\}_{m=1}^{N}} (k\overline{\gamma})^{-|\mathcal{X}\cup\mathcal{V}|+|\mathcal{E}|-|\mathcal{E}|} = (k'\overline{\gamma})^{-|\mathcal{X}\cup\mathcal{V}|} \end{aligned} \tag{28}$$

for some constant k' that absorbs the sum over all $\{\hat{x}^{(m)}\}_{m=1}^{N}$, because the terms in the sum no longer depend on $\{\hat{x}^{(m)}\}_{m=1}^{N}$; that is, the bound is independent of the errors after Phase 1, and so is its diversity order. □

3.2. Corollaries

Theorem 1 not only quantifies error performance bounds for our system, but also provides insight on how to design diversity-enabling mappings $\mathcal{M}_m$ for each S_m. The following examples illustrate these facts and establish desirable tradeoffs (summed up in Table 1) accounting for performance, complexity, spectral efficiency, and synchronism requirements.

Example 3 (repetition coding). In Section 2 we described a specific example in which each source transmits information of neighboring sources in separate time slots [cf. (6)]. Now, in view of Theorem 1, we can establish the following corollary.

Corollary 1. *Repetition coding defined by the encoding strategy in* (6) *and the detector in* (7) *achieves diversity* $d = 2$.

Proof. If x and $\widetilde{x}$ differ in at least two subblocks, we have $|\mathcal{X}| \geq 2$. In the worst-case event in which x differs from $\widetilde{x}$ in one unique sub-block, say the nth, we find $\mathcal{X} = \{n\}$. If we use repetition coding and permute symbols in one position as in (6), then $\mathcal{V} = \{\widetilde{n}\}$ with $\widetilde{n}\neq n$. Hence, the union of $\mathcal{X}$ and $\mathcal{V}$ has *at least* two elements and the detector in (7) achieves diversity $\min_{x,\widetilde{x}\neq x}\{|\mathcal{X}\cup\mathcal{V}|\} = 2$. □

Because information is forwarded without modification, this scheme can be interpreted as a relay scenario such as the one in [4]. Thus, Theorem 1 demonstrates diversity for classical relay schemes based on repetition coding. This result was already established in [4].

Repetition coding was the first reported cooperation strategy [3]. It features low-complexity detection and does not require symbol synchronization, because each source transmits frames over separate time slots. As demonstrated here, it can achieve diversity 2. With each source transmitting a frame of K symbols, and assuming that Phase 1 and Phase 2 have identical duration KN, the per-source bandwidth efficiency of repetition coding is $\eta = K/(KN+KN) = 1/(2N)$.

Example 4 (complex-field coding). In Section 2 we described the use of CFC to code blocks of symbols. In view of Theorem 1, we can now establish the following corollary.

Corollary 2. *For the distributed CFC strategy in* (8)*, if* $\boldsymbol{\theta}_m$ *is designed to guarantee that* $\boldsymbol{\theta}_m^T(\mathbf{p}_k - \widetilde{\mathbf{p}}_k)\neq 0$ *for any* $\mathbf{p}_k\neq\widetilde{\mathbf{p}}_k$ *and for any* m*, the detector in* (9) *achieves diversity* $d = N$.

Proof. If $\boldsymbol{\theta}_m^T(\mathbf{p}_k - \widetilde{\mathbf{p}}_k)\neq 0$ for any m, k, the matrix $(\mathbf{V} - \widetilde{\mathbf{V}})$ has (full) rank N; that is, $|\mathcal{V}| = N$. Thus, $\min_{x,\widetilde{x}\neq x}\{|\mathcal{X}\cup\mathcal{V}|\} = |\mathcal{V}| = N$. □

The condition $\boldsymbol{\theta}_m^T(\mathbf{p}_k - \widetilde{\mathbf{p}}_k)\neq 0$ is the so-called maximum-separability criterion. Designs for $\boldsymbol{\theta}_m$ are available in [15] in the context of MIMO systems with either systematic or numerically optimized constructions. Interestingly, a matrix $\boldsymbol{\Theta}$ enforcing maximum separability exists for any size N [15].

As with repetition coding, distributed CFC does not require synchronism at the symbol level. Likewise, the per-source bandwidth efficiency is also $\eta = K/(KN+KN) = 1/(2N)$, but higher diversity gains are possible.

Example 5 (distributed ST coding). Theorem 1 also allows us to analyze the performance of the distributed ST coding. Among the several options one may consider, we here analyze the performance of any generic ST code designed for a MISO system in which the number of transmit antennas equals the number of sources in our setup (N). Its implementation follows these steps. Suppose source S_m builds an $N\times 1$ vector $\mathbf{p}_k^{(m)} := [[\mathbf{x}_1^{(m)}]_k, \ldots, [\mathbf{x}_m]_k, \ldots, [\mathbf{x}_N^{(m)}]_k]^T$ after Phase 1 and maps it to a generic-size $T\times N$ matrix $\mathbf{T}_k^{(m)}$ (with rows denoting time and columns denoting space) using a generic ST mapping $\mathcal{M}_{\text{ST}}$. Source S_m builds $\mathbf{v}_m$ as follows:

$$\mathcal{M}_m:\ \mathbf{v}_m = \left[\left(\left[\mathbf{T}_1^{(m)}\right]_{:,m}\right)^T, \ldots, \left(\left[\mathbf{T}_K^{(m)}\right]_{:,m}\right)^T\right]^T, \tag{29}$$

Table 1: Comparison between distributed coding strategies.

	Diversity order (d)	BW efficiency η	Synchr. at symb. level
DSTC $N \times T$	from d_{ST} to $\min\{N, d_{\mathrm{ST}}+1\}$	$\frac{1}{N+T}$	Needed
Repetition	2	$\frac{1}{2N}$	Not needed
DCFC	N	$\frac{1}{2N}$	Not needed
DECC KP parity bits	$\min\left\{d_{\min}, 1+\left\lfloor N\left(1-\frac{K}{(K+P)\log_2\lvert\mathcal{A}_s\rvert}\right)\right\rfloor\right\}$	$\frac{1}{N+P}$	Not needed

that is, S_m concatenates the mth column of the K ST mapped matrices $\mathbf{T}_1^{(m)}, \ldots, \mathbf{T}_K^{(m)}$. By construction, $\mathbf{v}_m$ has size $KP \times 1$. Now, the following corollary assesses its performance when applied to our VAA setup.

Corollary 3. *Given a generic ST mapping $\mathcal{M}_{ST}$ that enables diversity d_{ST} in a MIMO system, its distributed implementation as in* (29) *can achieve diversity at least $d = d_{ST}$ and at most $d = \min\{N, d_{ST}+1\}$.*

Proof. If $\mathcal{M}_{\mathrm{ST}}$ enables diversity d_{ST}, it means that for any k, $\mathrm{rank}(\mathbf{T}_k - \widetilde{\mathbf{T}}_k) = d_{\mathrm{ST}}$. Now, adding up contributions from all sources, matrix $\mathbf{V}$ has size $KP \times N$ and is built as [cf. (29)]

$$\mathbf{V} = \left[\mathbf{T}_1^T, \ldots, \mathbf{T}_K^T\right]^T. \tag{30}$$

Equation (30) implies that for any k rank $\mathrm{rank}(\mathbf{V} - \widetilde{\mathbf{V}}) = \mathrm{rank}(\mathbf{T}_k - \widetilde{\mathbf{T}}_k) = d_{\mathrm{ST}}$. If, by construction, $\mathcal{M}_{\mathrm{ST}}$ is such that for some $\widetilde{x}$, a *worst-case* event $\mathcal{X} \in \mathcal{V}$ is possible, then $d = \min_{x,\widetilde{x}\neq x}\{|\mathcal{X}\cup\mathcal{V}|\} = |\mathcal{V}| = \mathrm{rank}(\mathcal{V}) = d_{\mathrm{ST}}$. If, instead, $\mathcal{M}_{\mathrm{ST}}$ is such that *for all* $\widetilde{x}\neq x$, $\mathcal{X}\cap\mathcal{V}\neq\varnothing$, then $d = \min_{x,\widetilde{x}\neq x}\{|\mathcal{X}\cup\mathcal{V}|\} = \min\{N, |\mathcal{X}| + |\mathcal{V}|\} = \min\{N, d_{\mathrm{ST}}+1\}$. □

Corollary 3 connects the diversity criteria for MIMO ST codes specified in, for example, [20], with its distributed *error-prone* implementation in multisource scenarios. It indeed demonstrates that a judicious distributed implementation of this ST code may increase its diversity by 1.

Compared to repetition coding or distributed CFC, the distributed ST codes described here require symbol-level synchronism to operate and their performance may degrade if sources are not perfectly synchronized [21, 22]. Simulations in Section 4 will consider this effect. For a general timespan of the code T, the bandwidth efficiency of this strategy is $\eta = 1/(N+T)$.

Example 6 (distributed error-correcting codes). Suppose that each source transmits

$$\mathcal{M}_m:\ \mathbf{v}_m = \left[\mathbf{0}_{(m-1)P}^T,\ \mathbf{v}_m'^T,\ \mathbf{0}_{(N-m)P}^T\right]^T, \tag{31}$$

and $\mathbf{v}_m'$ is a $P \times 1$ vector comprising parity check bits of the block $x^{(m)}$. Such mapping implements the distributed channel-coding strategy in [7, 14]. As depicted in Figure 3,

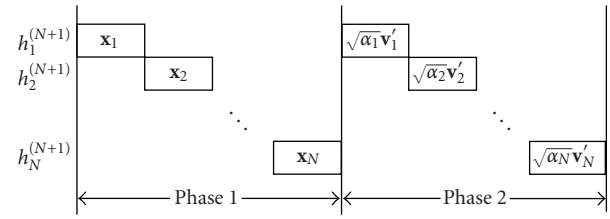

Figure 3: Time-division scheduling for N sources during Phase 1 and Phase 2.

the aggregate block sequence sent to the destination is $[\mathbf{x}_1, \ldots, \mathbf{x}_N, \widehat{\mathbf{v}}_1', \ldots, \widehat{\mathbf{v}}_N']$ and has size $N(K+P)$. The first NK symbols sent during Phase 1 then correspond to the systematic symbols and the NP symbols sent during Phase 2 comprise the parity-check portion of a generic ECC scheme. The following corollary states its performance.

Corollary 4. *The distributed implementation of ECC codes as described in* (31) *achieves diversity order $d = d_C$, where*

$$d_C \leq \min\left\{d_{\min}, 1+\left\lfloor N\left(1-\frac{K}{(K+P)\log_2\lvert\mathcal{A}_s\rvert}\right)\right\rfloor\right\} \tag{32}$$

and $d_{\min}$ is the minimum Hamming (free) distance of the ECC.

Proof. It is sufficient to observe that a sequence of systematic-plus parity-bits $[\mathbf{x}_1^T, \ldots, \mathbf{x}_N^T, (\mathbf{v}')_1^T, \ldots, (\mathbf{v}')_N^T]$, if transmitted over a point-to-point block-faded channel, achieves diversity d_C. This is indeed demonstrated in [16]. □

Notice that (32) is the Singleton bound. As shown in (32), the code rate and the constellation-employed affect the maximum achievable diversity order of coded transmissions over fading channels [16]. We further remark that in order to achieve diversity d_C, one has to judiciously design interleavers provided that systematic and parity bits are sent as shown in Figure 3.

Finally, note that DECC features low synchronism requirements (frame-level as in repetition and distributed CFC) and per-source bandwidth efficiency $\eta = 1/(N+P)$.

4. SIMULATIONS AND COMPARISONS

We present numerical simulations to test error performance of the proposed cooperative protocols. We employ binary phase-shift keying (BPSK). We suppose that all inter-source and source-destination links have the same average output SNR; that is, $\overline{\gamma}_n^{(m)} = \overline{\gamma}$, for all $n \in [1, N]$, $m \in [1, N+1]$.

4.1. Distributed coding strategies

We will compare the diversity order achieved by the encoding schemes in Examples 1, 2, 3, and 4 for different numbers of cooperating sources N.

4.1.1. Distributed orthogonal ST codes

Here we rely on the ST codes proposed in [23]. If $N = 2$, then $\widehat{\mathbf{p}}_k^{(m)}$ has size 2×1 and we map it to

$$\widehat{\mathbf{T}}_k = \begin{bmatrix} \left[\widehat{\mathbf{p}}_k^{(1)}\right]_1 & \left[\widehat{\mathbf{p}}_k^{(2)}\right]_2 \\ -\left(\left[\widehat{\mathbf{p}}_k^{(1)}\right]_2\right)^* & \left(\left[\widehat{\mathbf{p}}_k^{(2)}\right]_1\right)^* \end{bmatrix}. \tag{33}$$

The per-source bandwidth efficiency of this choice is $\eta = 1/4$. One can improve the rate without diversity loss by just sending

$$\widehat{\mathbf{T}}_k = \left[-\left(\left[\widehat{\mathbf{p}}_k^{(1)}\right]_2\right)^*, \left(\left[\widehat{\mathbf{p}}_k^{(2)}\right]_1\right)^* \right] \tag{34}$$

with per-source bandwidth efficiency $\eta = 1/3$. In (33) we have $|\mathcal{V}| = 2$ whereas in (34) $|\mathcal{V}| = 1$ but still $|\mathcal{X} \cup \mathcal{V}| = 2$. This same strategy can be generalized to $N > 2$ which corresponds to the ST orthogonal codes in [20].

Figure 4 depicts bit-error-rate (BER) as a function of the average SNR$\overline{\gamma}$ for different relay locations and schemes. Specifically, we compare (33) (LAR-DSTBC1), (34) (LAR-DSTBC2), and also [10] (DSTBC with no adaptation) and [11] (DSTBC with full channel knowledge at the destination). For reference, we also depict the BER when sources are not cooperating. Designs using LAR achieve diversity with different coding gains. Designs which do not exploit adaptivity suffer diversity loss. The performance is fairly close to that obtained with instantaneous channel knowledge [11].

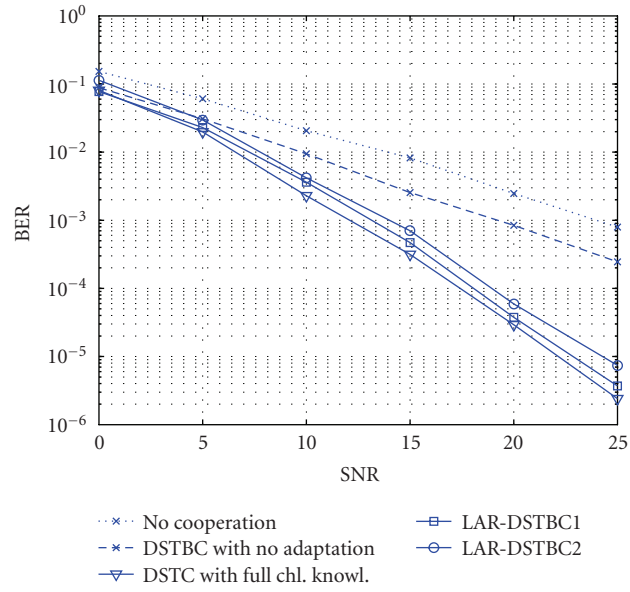

Figure 4: BER of DSTBC for $N = 2, 3$ sources and no cooperation.

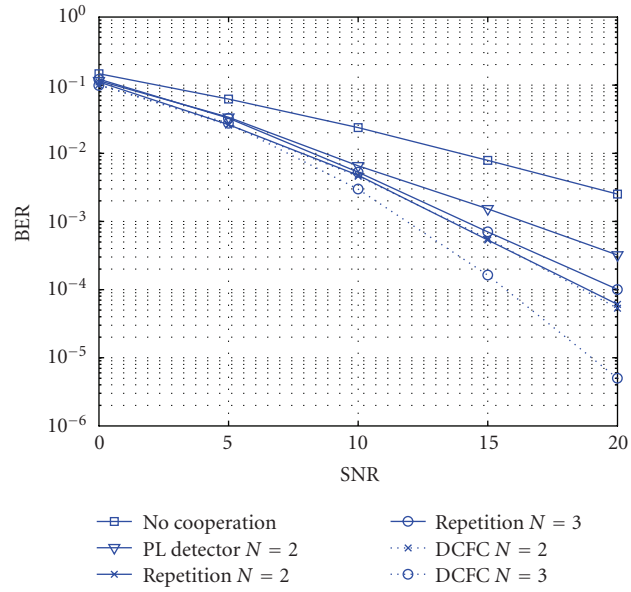

Figure 5: BER of DCFC versus repetition and PL relaying strategies for $N = 2, 3$ sources.

4.1.2. Repetition coding and distributed complex-field coding

Figure 5 shows the BER when employing DCFC, repetition coding, and the PL detector in [9] for $N = 1, 2, 3$ cooperating sources. The CFC matrix $\boldsymbol{\Theta}$ is chosen from [15]. For CFC and repetition-based transmissions, we employ the detectors in (9) and (7). For reference, we again depict the BER when sources are not cooperating. We can verify that, as established in Theorem 1, the slope of the BER varies with N when employing CFC and remains fixed to 2 when employing repetition coding with the same bandwidth efficiency. As a byproduct, we also outline the advantages of repetition-based link adaptation compared to [9]; whereas the former achieves diversity 2 in any scenario, the latter loses diversity when sources are sufficiently separated. As already mentioned, repetition coding is manifested in the well-known DF-relaying. This motivates us to also include comparisons with the coherent piecewise-linear (PL) detector of [9], which assumes that the average inter-source SNR is known at D.

4.1.3. Distributed convolutional codes

Figure 6 illustrates BER performance when employing the distributed convolutional codes (DCC) of [14] for $N = 2$ and $N = 4$ users. We employ blocks of size $K = 52$ bits encoded through a rate 1/2 convolutional code ($K = L$) with

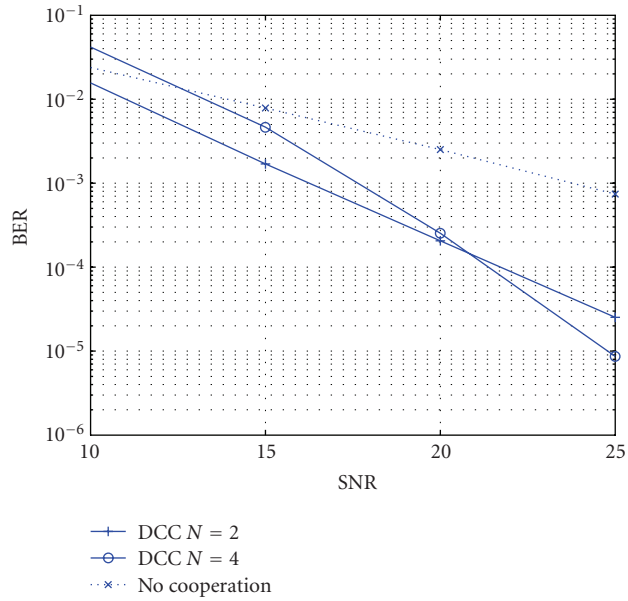

Figure 6: BER of DCC for $N = 2, 4$ sources.

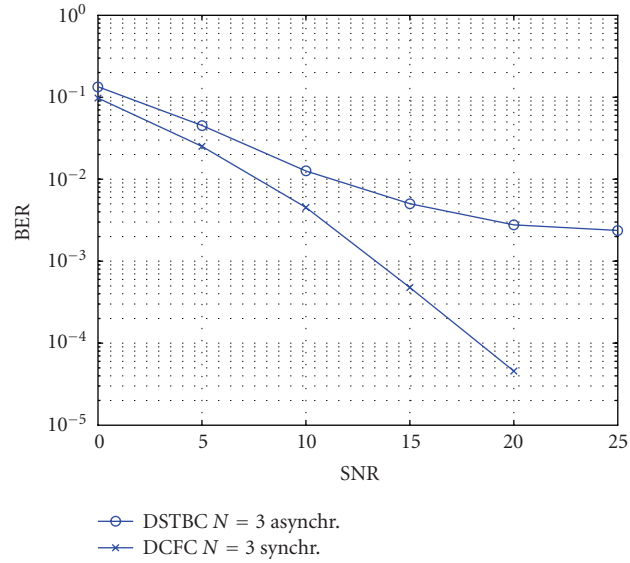

Figure 7: BER of DCFC versus DSTBC for $N = 3$ and asynchronous transmissions.

generator in octal form [5, 7] with Hamming (free) distance $d_{\text{free}} = 5$. According to (32), the achievable diversity orders are $d_C = 2$ for $N = 2$ and $d_C = 3$ for $N = 4$. Figure 6 confirms that diversity orders are achieved as predicted by Theorem 1. From the same figure we can also observe that coding gain is reduced. This can be due to the fact that highly corrupted blocks processed by the Viterbi decoder severely degrade its optimality at low SNRs.

4.2. Effect of synchronization

In the context of distributed setups, a fair comparison between distributed Alamouti, DCFC, and repetition coding should also account for synchronization issues. We fix the same bandwidth efficiency to be $\eta = 1/4$ and set the variation of timing offset to be uniformly distributed as $\mathcal{U}(-T_s, T_s)$ around the optimum sampling instant. We assume raised cosine pulses with roll-off factor $\beta = 0.22$. Figure 7 confirms the severe degradation that simultaneous transmissions suffer when accounting for mistiming across sources. Moreover, performance degradation increases with the number of users, which clearly offsets the potential diversity gains. We also show the performance of nonsimultaneous transmissions such as CFC, which do not experience this degradation.

4.3. CRC-aided retransmissions versus adaptive techniques

The advantages of MSC using SF as in [8] hinge upon the assumption of either error-free links between sources or, as is the case in practice, on correct error-detection decoding per frame. In this practical case, frames with errors are discarded and no signal is retransmitted. This strategy, however, can be inefficient at low SNR and/or when the CRC block size is large, because a single erroneous bit leads one to discard the entire block. To delineate this assessment, we set both strategies to use the same error-correction strategy. For the LAR, we set $\alpha_n = 1$ if no error is detected at user n; otherwise, the block is transmitted with α_n as in (13). This slight modification of our protocol, which we name LAR-SF, although not analytically proven here, can be reasonably expected to achieve full diversity. On the other hand, and for the sake of a fair comparison, we increase the average power of SF to match that of adaptive LAR-SF transmissions.

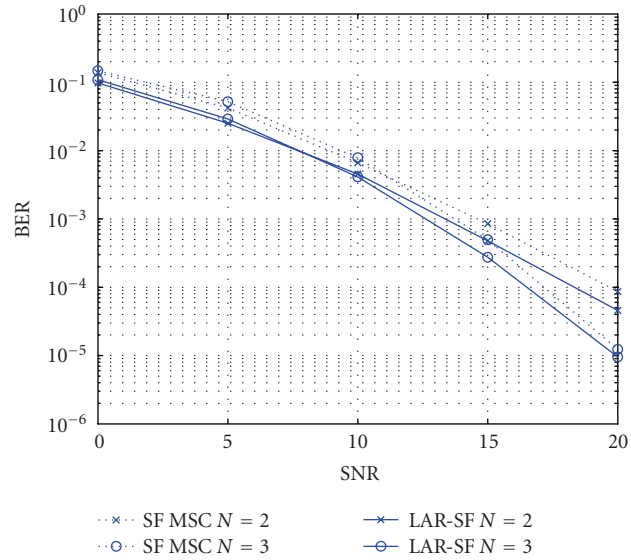

Figure 8: BER of adaptive versus selective retransmissions for packet length $K = 200$ bits and DCFC.

Figures 8 and 9 compare the BER of these strategies for block sizes of $K = 200$ and $K = 1024$ bits, respectively. As expected, both systems achieve full diversity. Moreover,

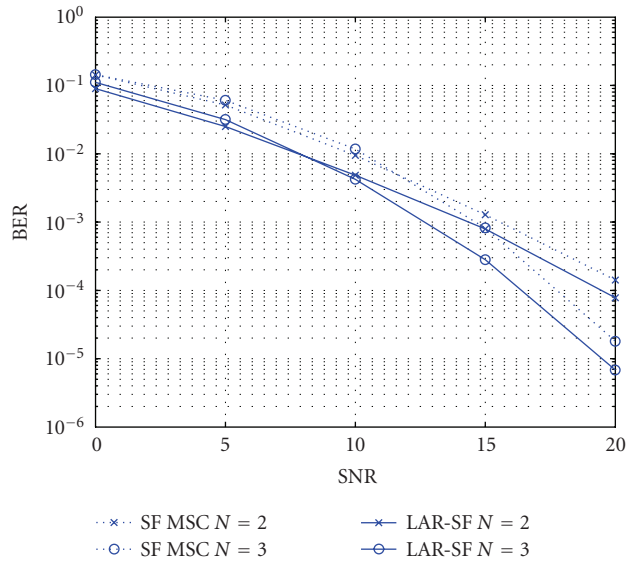

Figure 9: BER of adaptive versus selective retransmissions for packet length $K = 1024$ bits and DCFC.

link-adaptive transmissions exhibit larger coding gain, which corroborates the fact that discarding large packets renders SF strategies inefficient.

5. CONCLUSIONS

We have developed a link-adaptive relay protocol for use in multisource cooperative scenarios. General diversity performance was analyzed as a function of the rank properties of the distributed coding strategy. We included repetition coding, distributed CFC, distributed ST coding, and distributed ECC as particular cases of this general diversity analysis, concluding that the attainable diversity order is (i) 2 for repetition coding; (ii) N for DCFC; (iii) at least the same diversity order afforded by the ST codes in conventional antenna arrays when we use distributed ST coding; and (iv) for DECC the same diversity achieved by the ECC over an N-lag block fading channel. Simulations suggested that synchronization tasks are relevant to be included as part of the design of a VAA. In this context, we found that DCFC offers high-rate, full-diversity, and relaxed synchronization requirements.

APPENDICES

A. PROOF OF LEMMA 1(a)

The probability that S_m fails to detect the block $\mathbf{x}_n$ for all $n \neq m$ sent from S_n can be bounded as

$$\Pr\left\{\mathbf{x}_n \longrightarrow \hat{\mathbf{x}}_n^{(m)} \mid \mathcal{H}^{(s)}\right\} \leq Q\left(\left\|h_n^{(m)}\left(\mathbf{x}_n - \hat{\mathbf{x}}_n^{(m)}\right)\right\|\right), \tag{A.1}$$

where $Q(z) := 1/\sqrt{2\pi}\int_z^\infty \exp(-t^2/2)dt$. Considering that these are independent processes, the probability that S_m is in $\mathcal{E}$ is

$$\Pr\left\{x \longrightarrow \hat{x}^{(m)} \mid \mathcal{H}^{(s)}\right\} \leq \sum_{n=1, n\neq m}^{N} Q\left(\left\|h_n^{(m)}\left(\mathbf{x}_n - \hat{\mathbf{x}}_n^{(m)}\right)\right\|\right). \tag{A.2}$$

Letting $\delta_n^{(m)} := \sqrt{\sum_{k=1}^{K} |[\mathbf{x}_n]_k - [\hat{\mathbf{x}}_n^{(m)}]_k|^2}$ denote the squared Euclidean distance between $\mathbf{x}_n$ and $\hat{\mathbf{x}}_n^{(m)}$, and using the fact that function $Q(\cdot)$ is monotonically decreasing, its inner term can be bounded as $\|h_n^{(m)}(\mathbf{x}_n - \hat{\mathbf{x}}_n^{(m)})\| = \sqrt{\gamma_n^{(m)}(\delta_n^{(m)})^2} \geq \sqrt{\min_{m\neq n}\{\gamma_n^{(m)}\}\min_{m\neq n}\{(\delta_n^{(m)})^2\}}$. And thus,

$$\begin{aligned}&\sum_{m=1, m\neq n}^{N} Q\left(\left\|h_n^{(m)}\left(\mathbf{x}_n - \hat{\mathbf{x}}_n^{(m)}\right)\right\|\right)\\ &\qquad \leq (N-1)\exp\left(-\frac{1}{2}\min_{m\neq n}\left\{\gamma_n^{(m)}\right\}\min_{m\neq n}\left\{\left(\delta_n^{(m)}\right)^2\right\}\right),\end{aligned} \tag{A.3}$$

where we also used the fact that $Q(z) \leq \exp(-z^2/2)$. The probability that a set of sources $\mathcal{E}$ participates in error detection can be then readily bounded as

$$\begin{aligned}&\Pr\left\{x \longrightarrow \left\{\hat{x}^{(m)}\right\}_{m=1}^{N} \mid \mathcal{H}^{(s)}\right\}\\ &\leq \prod_{m\in\mathcal{E}} \Pr\left\{x \longrightarrow \hat{x}^{(m)} \mid \mathcal{H}^{(s)}\right\} \leq \kappa_1 \exp\left(-\kappa_2 \sum_{m\in\mathcal{E}} \min_{m\neq n}\left\{\gamma_n^{(m)}\right\}\right)\end{aligned} \tag{A.4}$$

for some finite constants κ_1 and κ_2.

B. PROOF OF LEMMA 1(b)

For compactness, we define $\overline{\mathbf{D}}_h^{(N+1)} := \operatorname{diag}(\mathbf{h}^{(N+1)}) \otimes \mathbf{I}_K$, $\overline{\mathbf{D}}_\alpha := \mathbf{D}_\alpha \otimes \mathbf{I}_K$, $\mathbf{y}^{(N+1,1)} := [(\mathbf{y}_1^{(N+1,1)})^T, \ldots, (\mathbf{y}_N^{(N+1,1)})^T]^T$ and $\mathbf{x} := [\mathbf{x}_1, \ldots, \mathbf{x}_N]^T$ and rewrite $\sum_{n=1}^{N}\|\mathbf{y}_n^{(N+1,1)} - \operatorname{diag}(\mathbf{x}_n)\mathbf{h}^{(N+1)}\|^2 = \|\mathbf{y}^{(N+1,1)} - \overline{\mathbf{D}}_h^{(N+1)}\mathbf{x}\|^2$. With these definitions, the probability of detection error in (5) is

$$\begin{aligned}&\Pr\left\{x, \left\{\hat{x}^{(m)}\right\}_{m=1}^{N} \longrightarrow \tilde{x} \mid \mathcal{H}^{(s)}, \mathcal{H}^{(d)}\right\}\\ &\quad = \Pr\left\{\left\|\mathbf{y}^{(N+1,1)} - \overline{\mathbf{D}}_h^{(N+1)}\mathbf{x}\right\|^2 + \left\|\mathbf{y}^{(N+1,2)} - \mathbf{V}\mathbf{D}_\alpha\mathbf{h}^{(N+1)}\right\|^2\right.\\ &\quad\quad > \left.\left\|\mathbf{y}^{(N+1,1)} - \overline{\mathbf{D}}_h^{(N+1)}\tilde{\mathbf{x}}\right\|^2 + \left\|\mathbf{y}^{(N+1,2)} - \tilde{\mathbf{V}}\mathbf{D}_\alpha\mathbf{h}^{(N+1)}\right\|^2\right\},\end{aligned} \tag{B.1}$$

where $\tilde{\mathbf{x}} := [\tilde{\mathbf{x}}_1^T, \ldots, \tilde{\mathbf{x}}_N^T]^T$. This probability of error can be written as $\Pr\{X > 0\}$, where

$$\begin{aligned}X :=\ &-2\operatorname{Re}\left\{\left(\mathbf{y}^{(N+1,1)}\right)^{\mathcal{H}}\overline{\mathbf{D}}_h^{(N+1)}(\mathbf{x} - \tilde{\mathbf{x}})\right\}\\ &- 2\operatorname{Re}\left\{\left(\mathbf{y}^{(N+1,2)}\right)^{\mathcal{H}}(\mathbf{V} - \tilde{\mathbf{V}})\mathbf{D}_\alpha\mathbf{h}^{(N+1)}\right\}\\ &+ \left\|\overline{\mathbf{D}}_h^{(N+1)}\mathbf{x}\right\|^2 - \left\|\overline{\mathbf{D}}_h^{(N+1)}\tilde{\mathbf{x}}\right\|^2 + \left\|\mathbf{V}\mathbf{D}_\alpha\mathbf{h}^{(N+1)}\right\|^2\\ &- \left\|\tilde{\mathbf{V}}\mathbf{D}_\alpha\mathbf{h}^{(N+1)}\right\|^2.\end{aligned} \tag{B.2}$$

Using $\mathbf{y}^{(N+1,1)} = \overline{\mathbf{D}}_h^{(N+1)}\mathbf{x} + \mathbf{w}^{(N+1,1)}$ and $\mathbf{y}^{(N+1,2)} = \hat{\mathbf{V}}\mathbf{D}_\alpha\mathbf{h}^{(N+1)} + \mathbf{w}^{(N+1,1)}$, it follows that X in (B.2) is a Gaussian random variable. Thus, the error probability is quantified by $\Pr\{X > 0\} = Q(-\mu/\sqrt{\sigma^2})$, where μ is its mean and σ^2 is its variance and is given by

$$\Pr\left\{x, \left\{\hat{x}^{(m)}\right\}_{m=1}^{N} \longrightarrow \tilde{x} \mid \mathcal{H}^{(s)}, \mathcal{H}^{(d)}\right\} = Q\left(\frac{\left|\left|\overline{\mathbf{D}}_h^{(N+1)}(\mathbf{x}-\tilde{\mathbf{x}})\right|\right|^2}{\sqrt{\left|\left|\overline{\mathbf{D}}_h^{(N+1)}(\mathbf{x}-\tilde{\mathbf{x}})\right|\right|^2 + \left|\left|(\mathbf{V}-\tilde{\mathbf{V}})\mathbf{D}_\alpha\mathbf{h}^{(N+1)}\right|\right|^2}} + \frac{\left|\left|(\hat{\mathbf{V}}-\tilde{\mathbf{V}})\mathbf{D}_\alpha\mathbf{h}^{(N+1)}\right|\right|^2 - \left|\left|(\hat{\mathbf{V}}-\mathbf{V})\mathbf{D}_\alpha\mathbf{h}^{(N+1)}\right|\right|^2}{\sqrt{\left|\left|\overline{\mathbf{D}}_h^{(N+1)}(\mathbf{x}-\tilde{\mathbf{x}})\right|\right|^2 + \left|\left|(\mathbf{V}-\tilde{\mathbf{V}})\mathbf{D}_\alpha\mathbf{h}^{(N+1)}\right|\right|^2}}\right). \tag{B.3}$$

The second term in the denominator of (B.3) can be expanded as $\|(\mathbf{V}-\tilde{\mathbf{V}})\mathbf{D}_\alpha\mathbf{h}^{(N+1)}\|^2 \le \|(\hat{\mathbf{V}}-\tilde{\mathbf{V}})\mathbf{D}_\alpha\mathbf{h}^{(N+1)}\|^2 + \|(\hat{\mathbf{V}}-\tilde{\mathbf{V}})\mathbf{D}_\alpha\mathbf{h}^{(N+1)}\|^2$. Defining the Euclidean distance $\delta_n := \sqrt{\sum_{k=1}^{K}|[\mathbf{x}_n]_k - [\tilde{\mathbf{x}}_n]_k|^2}$, we can write $\|\overline{\mathbf{D}}_h^{(N+1)}(\mathbf{x}-\tilde{\mathbf{x}})\|^2 = \sum_{n\in\mathcal{X}}\gamma_n^{(N+1)}\delta_n^2$, where we have used the definition of the set $\mathcal{X}$ in (12). Furthermore, one can bound this sum as

$$\sum_{n\in\mathcal{X}}\gamma_n^{(N+1)}\delta_n^2 \ge \sum_{n\in\mathcal{X}\cap\overline{\mathcal{E}}}\gamma_n^{(N+1)}\delta_n^2. \tag{B.4}$$

Now we turn our attention to $(\hat{\mathbf{V}}-\mathbf{V})$ and $(\hat{\mathbf{V}}-\tilde{\mathbf{V}})$. Matrix $(\hat{\mathbf{V}}-\mathbf{V})$ has *at most* $|\mathcal{E}|$ linearly independent columns indexed by $\mathcal{E}$; one can thus compute its singular value decomposition $(\hat{\mathbf{V}}-\mathbf{V}) = \mathbf{A}\boldsymbol{\Sigma}\mathbf{B}$ and choose $\mathbf{B}$ such that $[\mathbf{B}\mathbf{D}_\alpha\mathbf{h}^{(N+1)}]_n = \epsilon_n\sqrt{\alpha_n}h_n^{(N+1)}$ for $n \in \mathcal{E}$ and some nonzero constant ϵ_n, and bound

$$\left|\left|(\hat{\mathbf{V}}-\mathbf{V})\mathbf{D}_\alpha\mathbf{h}^{(N+1)}\right|\right|^2 \ge \sum_{n\in\mathcal{E}}\alpha_n\gamma_n^{(N+1)}\epsilon_n^2\lambda_n, \tag{B.5}$$

where λ_n is the associated singular value $\lambda_n := [\boldsymbol{\Sigma}]_{n,n}$. Likewise, $(\hat{\mathbf{V}}-\tilde{\mathbf{V}})$ has *at least* $|\mathcal{V}\cap\overline{\mathcal{E}}|$ linearly independent columns indexed by $\mathcal{V}\cap\overline{\mathcal{E}}$ and following the same reasoning as before, we can bound

$$\left|\left|(\hat{\mathbf{V}}-\tilde{\mathbf{V}})\mathbf{D}_\alpha\mathbf{h}^{(N+1)}\right|\right|^2 \le \sum_{n\in\mathcal{V}\cap\overline{\mathcal{E}}}\alpha_n\gamma_n^{(N+1)}\epsilon_n'^2\,\lambda_n' \tag{B.6}$$

for some nonzero $\epsilon_n'^2$ and λ_n'.

Inequalities (B.4) and (B.5) are lower bounds, whereas (B.6) is an upper bound. Using the fact that $Q((a-b)/\sqrt{a+b}) \le Q((c-d)/\sqrt{c-d})$ if $a \ge c$ and $b \le d$, we can rewrite (B.3) as

$$\Pr\{x, \{\hat{x}^{(m)}\}_{m=1}^{N} \longrightarrow \tilde{x} \mid \mathcal{H}^{(s)}, \mathcal{H}^{(d)}\} \le Q\left(\frac{B-B'}{\sqrt{B-B'}}\right), \tag{B.7}$$

where B denotes $\sum_{n\in\mathcal{X}\cap\overline{\mathcal{E}}}\gamma_n^{(N+1)}\delta_n^2 + \sum_{n\in\mathcal{X}\cap\overline{\mathcal{E}}}\alpha_n\gamma_n^{(N+1)}\epsilon_n^2\lambda_n$, B' denotes $\sum_{n\in\mathcal{E}}\alpha_n\gamma_n^{(N+1)}\epsilon_n'^2\lambda_n'$. Finally, noticing that sums over indexes $n \in \mathcal{X}\cap\overline{\mathcal{E}}$ and $n \in \mathcal{V}\cap\overline{\mathcal{E}}$ can be merged into a single sum with index $n \in (\mathcal{X}\cup\mathcal{V})\cap\overline{\mathcal{E}}$, and bounding with appropriate nonzero constants, one can readily arrive to (18).

ACKNOWLEDGMENTS

This work was supported through collaborative participation in the Communications and Networks Consortium sponsored by the US Army Research Laboratory under the Collaborative Technology Alliance Program, Cooperative Agreement no. DAAD19-01-2-0011. The US Government is authorized to reproduce and distribute reprints for Government purposes notwithstanding any copyright notation thereon. The work of the first author was supported by the Spanish Government Grant no. TEC2005-06766-C03-01/TCM.

REFERENCES

[1] A. Sendonaris, E. Erkip, and B. Aazhang, "User cooperation diversity—part I: system description," *IEEE Transactions on Communications*, vol. 51, no. 11, pp. 1927–1938, 2003.

[2] A. Sendonaris, E. Erkip, and B. Aazhang, "User cooperation diversity—part II: implementation aspects and performance analysis," *IEEE Transactions on Communications*, vol. 51, no. 11, pp. 1939–1948, 2003.

[3] J. N. Laneman and G. W. Wornell, "Distributed space-time-coded protocols for exploiting cooperative diversity in wireless networks," *IEEE Transactions on Information Theory*, vol. 49, no. 10, pp. 2415–2425, 2003.

[4] T. Wang, R. Wang, and G. B. Giannakis, "Smart regenerative relays for link-adaptive cooperation," to appear in *IEEE Transactions on Communications*.

[5] X. Deng and A. M. Haimovich, "Power allocation for cooperative relaying in wireless networks," *IEEE Communications Letters*, vol. 9, no. 11, pp. 994–996, 2005.

[6] M. O. Hasna and M.-S. Alouini, "Optimal power allocation for relayed transmissions over Rayleigh-fading channels," *IEEE Transactions on Wireless Communications*, vol. 3, no. 6, pp. 1999–2004, 2004.

[7] O. Shalvi, "Multiple source cooperation diversity," *IEEE Communications Letters*, vol. 8, no. 12, pp. 712–714, 2004.

[8] A. Ribeiro, R. Wang, and G. B. Giannakis, "Multi-source cooperation with full-diversity spectral-efficiency and controllable-complexity," *IEEE Journal on Selected Areas in Communications*, vol. 25, no. 2, pp. 415–425, 2007.

[9] D. Chen and J. N. Laneman, "Modulation and demodulation for cooperative diversity in wireless systems," *IEEE Transactions on Wireless Communications*, vol. 5, no. 7, pp. 1785–1794, 2006.

[10] G. Scutari, S. Barbarossa, and D. Ludovici, "Cooperation diversity in multihop wireless networks using opportunistic driven multiple access," in *Proceedings of the IEEE International Workshop on Signal Processing Advances for Wireless Communications*, pp. 170–174, Rome, Italy, June 2003.

[11] P. A. Anghel, G. Leus, and M. Kaveh, "Distributed space-time cooperative systems with regenerative relays," *IEEE Transactions on Wireless Communications*, vol. 5, no. 11, pp. 3130–3141, 2006.

[12] T. E. Hunter and A. Nosratinia, "Diversity through coded cooperation," *IEEE Transactions on Wireless Communications*, vol. 5, no. 2, pp. 283–289, 2006.

[13] S. M. Alamouti, "A simple transmit diversity technique for wireless communications," *IEEE Journal on Selected Areas in Communications*, vol. 16, no. 8, pp. 1451–1458, 1998.

[14] R. Wang, W. Zhao, and G. B. Giannakis, "Multi-source cooperative networks with distributed convolutional coding," in *Proceedings of the 39th Asilomar Conference on Signals, Systems and Computers*, pp. 1056–1060, Pacific Grove, Calif, USA, October 2005.

[15] Y. Xin, Z. Wang, and G. B. Giannakis, "Space-time diversity systems based on linear constellation precoding," *IEEE Transactions on Wireless Communications*, vol. 2, no. 2, pp. 294–309, 2003.

[16] R. Knopp and P. A. Humblet, "On coding for block fading channels," *IEEE Transactions on Information Theory*, vol. 46, no. 1, pp. 189–205, 2000.

[17] G. B. Giannakis, Z. Liu, X. Ma, and S. Zhou, *Space-Time Coding for Broadband Wireless Communications*, John Wiley & Sons, New York, NY, USA, 2006.

[18] J. G. Proakis, *Digital Communications*, McGraw-Hill Higher Education, New York, NY, USA, 4th edition, 2001.

[19] T. Wang and G. B. Giannakis, "High-throughput cooperative communications with complex field network coding," in *Proceedings of the 41st Annual Conference on Information Sciences and Systems (CISS '07)*, pp. 253–258, Baltimore, MD, USA, March 2007.

[20] V. Tarokh, N. Seshadri, and A. R. Calderbank, "Space-time codes for high data rate wireless communication: performance criterion and code construction," *IEEE Transactions on Information Theory*, vol. 44, no. 2, pp. 744–765, 1998.

[21] S. Jagannathan, H. Aghajan, and A. Goldsmith, "The effect of time synchronization errors on the performance of cooperative MISO systems," in *Proceedings of IEEE Global Telecommunications Conference Workshops (GLOBECOM '04)*, pp. 102–107, Dallas, Tex, USA, November 2004.

[22] X. Li, F. Ng, J.-T. Hwu, and M. Chen, "Channel equalization for STBC-encoded cooperative transmissions with asynchronous transmitters," in *Proceedings of the 39th Asilomar Conference on Signals, Systems and Computers*, pp. 457–461, Pacific Grove, Calif, USA, October-November 2005.

[23] V. Tarokh, H. Jafarkhani, and A. R. Calderbank, "Space-time block codes from orthogonal designs," *IEEE Transactions on Information Theory*, vol. 45, no. 5, pp. 1456–1467, 1999.